Premature senescence is a major response to DNA cross-linking agents in BRCA1-defective cells: implication for tailored treatments of BRCA1 mutation carriers

Manuela Santarosa, Laura Del Col, Elena Tonin, Angela Caragnano, Alessandra Viel, and Roberta Maestro

Experimental Oncology 1, Centro di Riferimento Oncologico, Istituto Di Ricovero e Cura a Carattere Scientifico, National Cancer Institute, Aviano, Italy

Abstract

BRCA1-associated tumors are characterized by an elevated genomic instability and peculiar expression profiles. Nevertheless, tailored treatments for BRCA1 mutation carriers have only been partially investigated up to now. The implementation of therapeutic strategies specific for these patients has been in part hindered by the paucity of proper preneoplastic and neoplastic BRCA1-deficient tumor cell models. In this study, we took advantage of the RNA interference technology to generate a series of partially transformed (HBL100) and tumorigenic (MCF7 and T47D) breast cancer cell lines in which BRCA1 expression was silenced at different levels. These cell models were probed by clonogenic assay for their response to several DNA-damaging agents commonly used in cancer therapy (mitomycin C, cisplatin, doxorubicin, and etoposide). Our models confirmed the peculiar sensitivity to interstrand cross-link inducers associated with BRCA1 deficiency. Intriguingly, the increased sensitivity to these compounds displayed by BRCA1-defective cells was not correlated with the extent of apoptotic cell death but rather associated to an increased fraction of growth-arrested, enlarged, multinucleated β-galactosidase–positive senescent cells. Overall, our results support a role for BRCA1 in the regulation of interstrand cross-link–induced premature senescence and suggest a reconsideration of the therapeutic power of mitomycin/platinum-based treatments in BRCA1 carriers. Moreover, our data further prompt the setup of strategies for the imaging of the senescence response *in vivo*. [Mol Cancer Ther 2009;8(4):844–54]

Received 10/3/08; revised 1/19/09; accepted 2/3/09.

Grant support: Italian Association for Cancer Research and Fondazione CRUP. L. Del Col was supported by the Fondazione Italiana per la Ricerca sul Cancro.

The costs of publication of this article were defrayed in part by the payment of page charges. This article must therefore be hereby marked *advertisement* in accordance with 18 U.S.C. Section 1734 solely to indicate this fact.

Editor's Note: A question was raised regarding the content of a figure in this article. The editors reviewed this inquiry in 2019 and determined that no action was needed at that time.

Requests for reprints: Roberta Maestro, Experimental Oncology 1, Centro di Riferimento Oncologico, Istituto Di Ricovero e Cura a Carattere Scientifico, National Cancer Institute, via F. Gallini 2, Aviano 33081 PN, Italy. Phone: 39-0434-659670; Fax: 39-0434-659659. E-mail: maestro@cro.it

doi:10.1158/1535-7163.MCT-08-0951

Introduction

BRCA1 germ-line mutations are responsible for a large proportion of hereditary breast and ovarian cancers. A striking phenotype of BRCA1-associated tumors and corresponding cell models is a high degree of genomic instability, extensive chromosomal aberrations, and aneuploidy. These phenomena may be ascribed to the role that BRCA1 is thought to play in maintaining genomic integrity (1). Indeed, BRCA1 is involved in a plethora of cellular processes, including DNA damage response (1, 2), chromatin remodeling (3), XIST-dependent X-chromosome silencing (4), telomere protection (5, 6), and transcription elongation (7). In particular, robust evidence indicates that BRCA1 is involved in homologous recombination–mediated DNA repair of double-strand breaks (1). In line with its pleiotropic functions, BRCA1 has been found to complex with a wide range of proteins involved in cell cycle checkpoint control and DNA repair, such as ATM/ATR, BRCA2, CtIP, Chk1/Chk2, p53, and Rad50-Mre11-Nbs1 (8, 9). Moreover, BRCA1 is required for ATM- and ATR-mediated phosphorylation/activation of Chk2, Nbs1, and p53 after IR or UV exposure (10, 11). Still, the exact mechanism of action of BRCA1 has not been established yet. Furthermore, despite carriers of BRCA1 mutations develop breast tumors with peculiar molecular profiles, tailored treatments for this category of patients have only been partially investigated (12, 13).

Most of our knowledge on the role of BRCA1 in the drug response of breast cancer cells comes from studies done on murine cell models or on a breast cancer cell line (HCC1937) obtained from a carrier of BRCA1 mutation (14–19). The analysis of these BRCA1-defective models has suggested an increased sensitivity to specific categories of chemotherapeutic agents. In particular, BRCA1 deficiency seems to sensitize cells to alkylating agents that induce intrastrand and interstrand cross-links (ICL), phenomenon that has been associated to the role played by BRCA1 in homologous recombination (14, 19), whereas contradictory results have been instead obtained with other chemotherapeutics such as the topoisomerase II inhibitors (15, 16, 19). The molecular bases of this characteristic response and how the increased susceptibility of BRCA1-defective tumor cells to ICL inducers may be

exploited to improve the treatment of BRCA1 patients still require investigations.

In this study, we took advantage of the RNA interference technology to generate several isogenic breast cancer cell lines in which BRCA1 expression was silenced at different levels. Our models were then challenged with several different chemotherapeutics and analyzed for cell survival. The use of clonogenic assay, which, being a long-term assay, consents not only the detection of acute cell death but also the evaluation of chronic proliferative damages, allowed us to explore the full spectrum of cell responses to these drugs.

Our study confirmed the high sensitivity to both mitomycin C (MMC) and CDDP of BRCA1-defective cells. Intriguingly, we found that this hypersensitivity was not associated to an enhanced apoptotic response but rather to the induction of premature senescence. Our results support a role for BRCA1 in the regulation of DNA damage–induced premature senescence and disclose new therapeutic opportunities for the treatment of BRCA1 carriers.

Materials and Methods

Cell Culture

HBL100 cell line was purchased from Interlab Cell Line Collection. HBL100 are normal breast cells transduced with the SV40 early region. These cells, in which the p53 and RB pathway are inactivated by the SV40 large T antigen, are considered a partially transformed breast cancer cell model. HCC1937 and the derivative HCC+BR (HCC1937 transfected with full-length BRCA1), a kind gift from Dr. D.P. Harkin (Centre Cancer Research and Cell Biology, Queen's University of Belfast, Northern Ireland; ref. 15), carry a homozygous insertion in the *BRCA1* gene (5382insC) and a truncating mutation (R306X) in p53. MCF7 and T47D cell lines were purchased from the American Type Culture Collection and are p53 wild-type and p53 mutant (L194F), respectively.[1]

HBL100 and T47D cell lines were grown in MEM (Life Technologies, Invitrogen) supplemented with 10% of fetal bovine serum (Life Technologies, Invitrogen); MCF7 and HCC1937 cell lines were maintained in RPMI 1640 supplemented with 10% and 20% fetal bovine serum, respectively (Life Technologies, Invitrogen). HCC+BR cell line was grown in HCC1937 medium supplemented with 0.2 mg/mL G418 (Life Technologies, Invitrogen).

Generation of BRCA1-Silenced Cell Lines

BRCA1-silenced cell clones (HBLpS-BR, MCF7pS-BR, and T47DpS-BR) were obtained form HBL100, MCF7, and T47D cell lines by stable transfection with gene-specific pSUPER constructs. *BRCA1*-specific pSUPER constructs pSUPER-BRCA1 and pSUPER-BRCA1b were produced expressing the RNA interference target sequences 5′-GAGGAGCTCATTAAGGTTG (mapping on exon 15) and 5′-GTAGCTGATGTATTGGACG (mapping on exon 11), respectively. Cell lines were transfected with pSUPER-BRCA1 or pSUPER (scrambled vector as a control: 5′-CATGCCTGATCCGCTAGTC) and a vector expressing neomycin resistance (pcDNA3.1, Invitrogen) at a ratio of 20:1 (pSUPER/pcDNA3.1) using the FuGene6 reagent (Roche) according to the manufacturer's instructions. After selection with G418 (Invitrogen), resistant clones were checked for the presence of pSUPER-BRCA1 or pSUPER by PCR with T3 and T7 primers. BRCA1 silencing was assessed by real-time PCR and Western blot. For real-time PCR, RNA was extracted with the Trizol reagent (Invitrogen) and then treated with RQ1 RNase-free DNase (Promega). Reverse transcription was done with Expand reverse trascriptase (Boehringer Mannheim). Real-time quantitative PCR was done in triplicate with the ABI Prism 7900HT Sequence Detection System (PE Biosystems) and the SYBR Green PCR Master Mix (Applied Biosystems). Primers were as follows: *BRCA1*, 5′-TTGCAGTGTGGGAGATCAAG (forward) and 5′-TGTTCTCATGCTGTAATGAGC (reverse). Geometric average of four different housekeeping genes was used for normalization: *18S rRNA*, 5′-GTAACCCGTTGAACCCCATT (forward) and 5′-CCATCCAATCGGTAGTAGCG (reverse); β-actin, 5′-CACCTTCTACAATGAGCTGCGT (forward) and 5′-AGCCTGGATAGCAACGTACATG (reverse); *β2-microglobulin*, 5′-GAGTATGCCTGCCGTGTG (forward) and 5′-AATCCAAATGCGGCATCT (reverse); and *glyceraldehyde-3-phosphate dehydrogenase*, 5′-GAAGGTGAAGGTCGGAGTC (forward) and 5′-GAAGATGGTGATGGGATTTC (reverse).

Western Blot Analysis and Antibodies

Western blotting was done on cell protein lysates [50 mmol/L Tris-HCl (pH 7.4), 150 mmol/L NaCl, 0.20% Triton X-100, 0.30% NP40, 2 mmol/L EGTA, 2 mmol/L EDTA, 25 mmol/L NaF, 25 mmol/L glycerol-2-phosphate, 2 mmol/L sodium orthovanadate, 0.1 mmol/L phenylmethylsulfonyl fluoride, and Complete protease inhibitor cocktail (Roche)] using antibodies reactive to BRCA1 (Ab-1; Oncogene), poly(ADP-ribose) polymerase full-length 116 kDa and its 85-kDa cleaved product (F-2; Santa Cruz Biotechnology), β-tubulin (H-235; Santa Cruz Biotechnology), CDKN1A ($p21^{cip1/waf1}$; BD Biosciences), and α-actin (1A4; Santa Cruz Biotechnology). Anti-rabbit and anti-mouse secondary antibodies conjugated with IR Dye 800 (Rockland) or Alexa Fluor 680 (Molecular Probes) were used as required. The Odyssey IR imaging system (LI-COR Biosciences) was used for blot visualization and quantification.

Clonogenic Assays

Sensitivity to chemotherapeutics was evaluated by clonogenic assay. Exponentially growing cells were plated into 60-mm dishes at a range of density and incubated overnight. The following day, cells were incubated in cell medium supplemented with the reported concentration doses of MMC (Kyowa), cisplatin (CDDP, Platamine, Pharmacia & Upjohn), doxorubicin (Adriblastin, Pharmacia), and etoposide (Teva Pharma). After 24 h of incubation, cells were washed and incubated with fresh clear medium for further 2 wk to allow colony formation. Plates were then washed with PBS and stained with 0.05% of crystal violet in 70% ethanol. Clusters containing >50 cells were scored as colonies. All clonogenic assays were done at least

[1] http://www.sanger.ac.uk/

thrice in triplicate. The plating efficiency is calculated as the number of colonies per plate divided by the number of cells originally seeded times 1,000. The surviving fraction for a given dose was calculated as the ratio between the plating efficiency of treated and untreated cells. SigmaPlot was used to fit curves to the mean surviving fraction using a sigmoidal dose-response equation and to calculate the IC_{50}.

Alkaline Comet Assay

To quantify the level of induced ICLs, we used a modified alkaline version of the Comet assay as described by Hartley et al. (20). In particular, HBL100 derivative clones were treated with 5 μmol/L MMC for 1 h, shifted to drug-free medium from 0 to 24 h, and then collected and kept in ice. DNA was then sheared by irradiating the pellet with a ^{137}Cs γ-irradiator (10 Gy). For each assay, 30,000 cells were added with 3 volumes of 1% low–melting point agarose (Invitrogen), quickly pipetted onto a fully frosted microscope slides (Electron Microscopy Sciences) previously covered with 1% normal–melting point agarose. Slides were then immersed in cold lysis solution [2.5 mol/L NaCl, 100 mmol/L Na_2EDTA, 10 mmol/L Tris (pH 10), 1% Triton X-100] for 2 h at 4°C. After lysis, slides were placed for 30 min in a horizontal gel electrophoresis tank filled with cold electrophoresis buffer [300 mmol/L NaOH, 1 mmol/L Na_2EDTA (pH >13)] to allow DNA unwinding to occur. Electrophoresis was then conducted at 300 mA for 40 min. Slides were neutralized with 0.4 mol/L Tris (pH 7.5) and stained with SYBR Green I. Per slide, 50 images were randomly captured by fluorescence microscopy and analyzed using VisCOMET software (Impuls). Variations in tail extent moment (TEM) were calculated as follows:

$$\%\ \mathrm{TEM} = \frac{(\mathrm{TEM\ sample} - \mathrm{TEM\ untreated\ sample}) \times 100}{(\mathrm{TEM\ IR\ sample} - \mathrm{TEM\ untreated\ sample})}$$

where TEM untreated sample indicated sample treated neither with MMC nor with radiation and TEM IR indicated sample MMC untreated but irradiated.

γH2AX and RAD51 Focus Formation

HBLpS and HBLpS-BR cell lines were cultured on microscopy slides for 24 h with 0.5 μmol/L MMC (0 h). For H2AX phosphorylation (γH2AX) assay, cells were then washed and left to recover in drug-free medium for 48 h. Cells were then fixed in 4% paraformaldehyde/PBS, permeabilized with 0.2% Triton X-100/PBS, and stained with rabbit anti-γH2AX polyclonal antibody (Upstate) or anti-RAD51 monoclonal mouse antibody (Abcam) at 4°C overnight. After washing, the primary antibodies were visualized with Alexa Fluor 594 anti-rabbit IgG (Molecular Probes, Invitrogen) or FITC anti-mouse IgG (Vector Laboratories). Slides were then mounted with 4′,6-diamidino-2-phenylindole mounted medium (Vector Laboratories) and examined under a fluorescence microscope. The experiments were done in triplicate and at least 100 random nuclei were counted by two independent readers. A positive score was given for more than five foci per nucleus.

Detection of Apoptosis

Caspase-3 and caspase-7 activities were measured using Caspase-Glo 3/7 assay kit (Promega). Briefly, 4,000 cells were plated in triplicate on a 96-well plate (Cultureplate96, Perkin-Elmer) and incubated overnight to allow cells to adhere. Cells were then incubated for 48 h with drug-free medium or medium supplemented with the reported dose of MMC, CDDP, or etoposide and then processed according to the manufacturer's protocol. Caspase activity was measured using a luminometer (TopCount 9906, Perkin-Elmer). Values were normalized for the plating efficiency at 24 h.

Poly(ADP-ribose) polymerase cleavage was evaluated by Western blotting on lysates from cells treated with the reported drug dosages for 48 h. γ-Irradiated HBL100 cells were used as positive control. Cells were γ-irradiated using a ^{137}Cs γ-irradiator for a total of 10 Gy, harvested at 15 h after irradiation, and processed as described.

Detection of Senescence

Senescence-associated β-galactosidase activity (pH 6) was assessed using standard protocols on cells processed as described in clonogenic assay. The extent of senescence was calculated as a ratio of senescence-associated β-galactosidase–positive cells (mean of at least three independent experiments) over the plating efficiency of untreated cells. The Fisher's test was used to assess statistical significance.

Flow Cytometry

For analysis of DNA content, MMC-treated and MMC-untreated cells were harvested with trypsin, washed in PBS, and fixed in 70% ethanol at −20°C. Fixed cells were rehydrated with PBS, stained with propidium iodide, and then analyzed (Cytomics F500, Beckman Coulter).

Bromodeoxyuridine (BrdUrd) incorporation was evaluated using the FITC BrdU Flow kit (BD Biosciences) according to the manufacturer's protocol.

Results

Drug Sensitivity in BRCA1-Silenced Cells

To gain insights on the role of BRCA1 in the response to chemotherapy, we generated three new breast cancer cell models defective for BRCA1 expression. In particular, the partially transformed HBL100 and the tumorigenic MCF7 and T47D breast cancer cell lines were stably transfected with pSUPER-BRCA1 vectors. Transfection with scrambled vector served as a control.

In HBL100, most shBRCA1-transfected colonies showed down-regulation of BRCA1, with 80% to 90% reduction in protein expression. Two clones with these features were then selected for further characterization (HBLpS-BR1 and HBLpS-BR2). In contrast, in MCF7 and T47D, only few colonies showed reduction in BRCA1 expression, which was only partial in most cases. Two MCF7 clones with a residual expression of ~25% and ~50% (MCF7pS-BR1 and MCF7pS-BR2) and one T47D clone (~50% residual expression) were then selected (Fig. 1). Nontransfected cells and pools of pSUPER-scrambled vector–transfected cells (HBLpS, MCF7pS, and T47DpS) were used as controls.

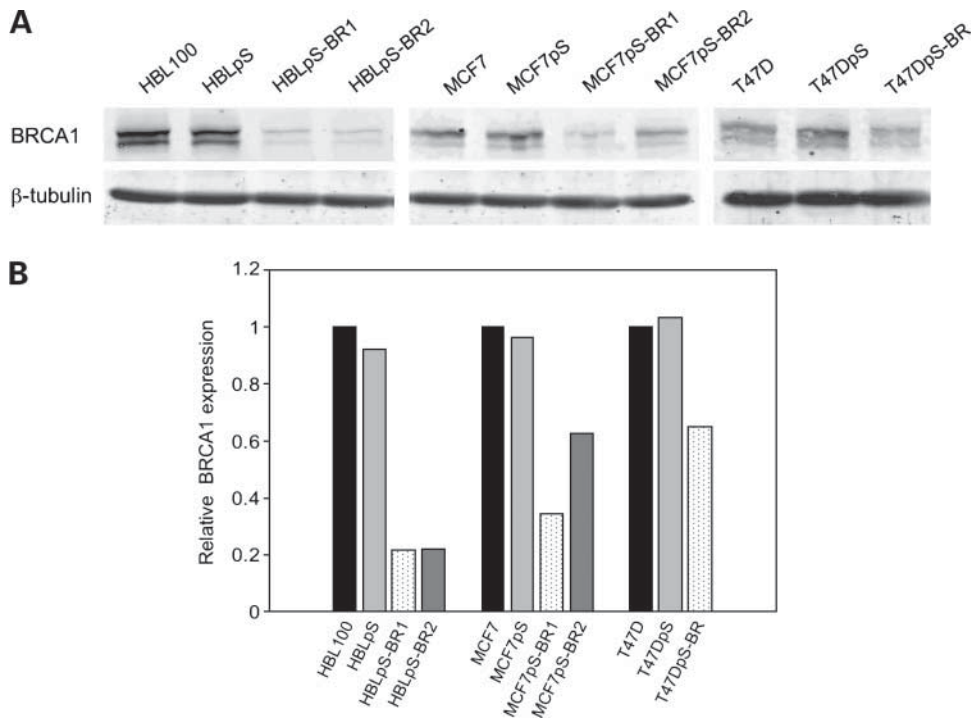

Figure 1. BRCA1-silenced human breast cell lines. **A,** Western blot analysis showing BRCA1 silencing in HBL100 (HBLpS-BR1 and HBLpS-BR2), MCF7 (MCF7pS-BR1 and MCF7pS-BR2), and T47D (T47DpS-BR) cell clones. Parental cell lines and scrambled vector–transfected cells (HBLpS, MCF7pS, and T47DpS) are shown as reference controls. Sample loading was normalized for β-tubulin. **B,** BRCA1 silencing was confirmed also by real-time quantitative PCR. The plot shows the expression ratio between BRCA1-silenced clones and corresponding parental cell line.

Sensitivity to MMC, cisplatin (CDDP), doxorubicin, or etoposide was then assessed in our cell models by clonogenic assay, which allows the contemporary evaluation of both survival capacity and proliferation power, and compared with HCC1937 BRCA1-proficient and BRCA1-deficient cells.

Similar to data previously reported for HCC1937 (15, 16), silencing of BRCA1 produced augmented sensitivity to ICL inducers in all the cell models analyzed, as indicated by the IC_{50} values (Fig. 2A and B; Table 1). In particular, after treatment with increasing doses of MMC and CDDP, cell survival was noticeably reduced in the cell models exhibiting a more marked reduction in BRCA1 expression, with the BRCA1-null HCC1937 showing the highest sensitivity. The increased sensitivity observed in BRCA1-silenced cells was not due to differences in the proliferation rate because silenced and nonsilenced cells displayed comparable doubling times in standard conditions (data not shown). Furthermore, nontransfected or scrambled-transfected cells showed no difference in terms of sensitivity to any of the drugs used in this study.

In contrast to previous reports for ICL inducers, loss of BRCA1 expression did not affect the response to topoisomerase II inhibitors. In fact, no significant difference was observed in the sensitivity to etoposide between BRCA1-deficient and BRCA1-proficient cells (Fig. 3A; Table 1). Similar results were observed also for doxorubicin, with the only exception of the highly silenced MCF7pS-BR1 clone for which a partial reduction in IC_{50} was observed (Fig. 3B; Table 1).

Overall, our results support the notion that BRCA1 is a key mediator of the cell response to ICL inducers, whereas other genetic factors are likely to play a major role in the response to topoisomerase II inhibitors.

ICL Repair in BRCA1-Defective Cells

In the light of the association between BRCA1 and DNA repair, we sought to investigate if the hypersensitivity to ICL inducers observed in our cell systems actually related to faults in the processing of DNA damage.

Typically, the repair of ICLs involves the formation of DNA double-strand breaks (incision step) followed by a homologous recombination event (21). To investigate whether ICL inducer hypersensitivity was due to alterations in the incision step, the unhooking efficiency of MMC-induced ICLs was analyzed in HBL100 derivative cells. ICL induction and unhooking was evaluated at single-cell level using the alkaline Comet assay according to Hartley et al. (20). In this assay, MMC-treated cells are γ-irradiated (10 Gy) to induce random DNA strand breakage. In the presence of ICLs, the migration of the irradiated broken DNA is retarded during electrophoresis, resulting in a reduced tail moment (TEM) in MMC-treated cells compared with the untreated controls. The reduction in TEM is proportional to the level of induced ICL. The ability of cells to unhook cross-linking (incision step) can therefore be monitored as an increase in TEM following a repair step in drug-free medium. MMC alone, in the absence of radiation-induced breakage, did not alter significantly the TEM of either cell line compared with untreated cells. As expected, TEM was significantly increased by γ-radiation (radiation alone), but no difference was observed between HBLpS-BR and HBLpS cells (Supplementary Fig. S1).[2] After MMC pulse

[2] Supplementary data for this article are available at Molecular Cancer Therapeutics Online (http://mct.aacrjournals.org/).

(5 μmol/L for 1 hour) and radiation-induced breakage, at time 0 TEM was still comparable in HBLpS and HBLpS-BR cell lines (Fig. 4A; Supplementary Fig. S1).[2] In particular, both cell lines showed a TEM that was roughly corresponding to 50% of TEM observed in control cells (100%). Following 24 hours in drug-free medium to allow cells to repair the damage, TEM increased in both cell systems, indicating that the incision step was not affected by BRCA1 deficiency.

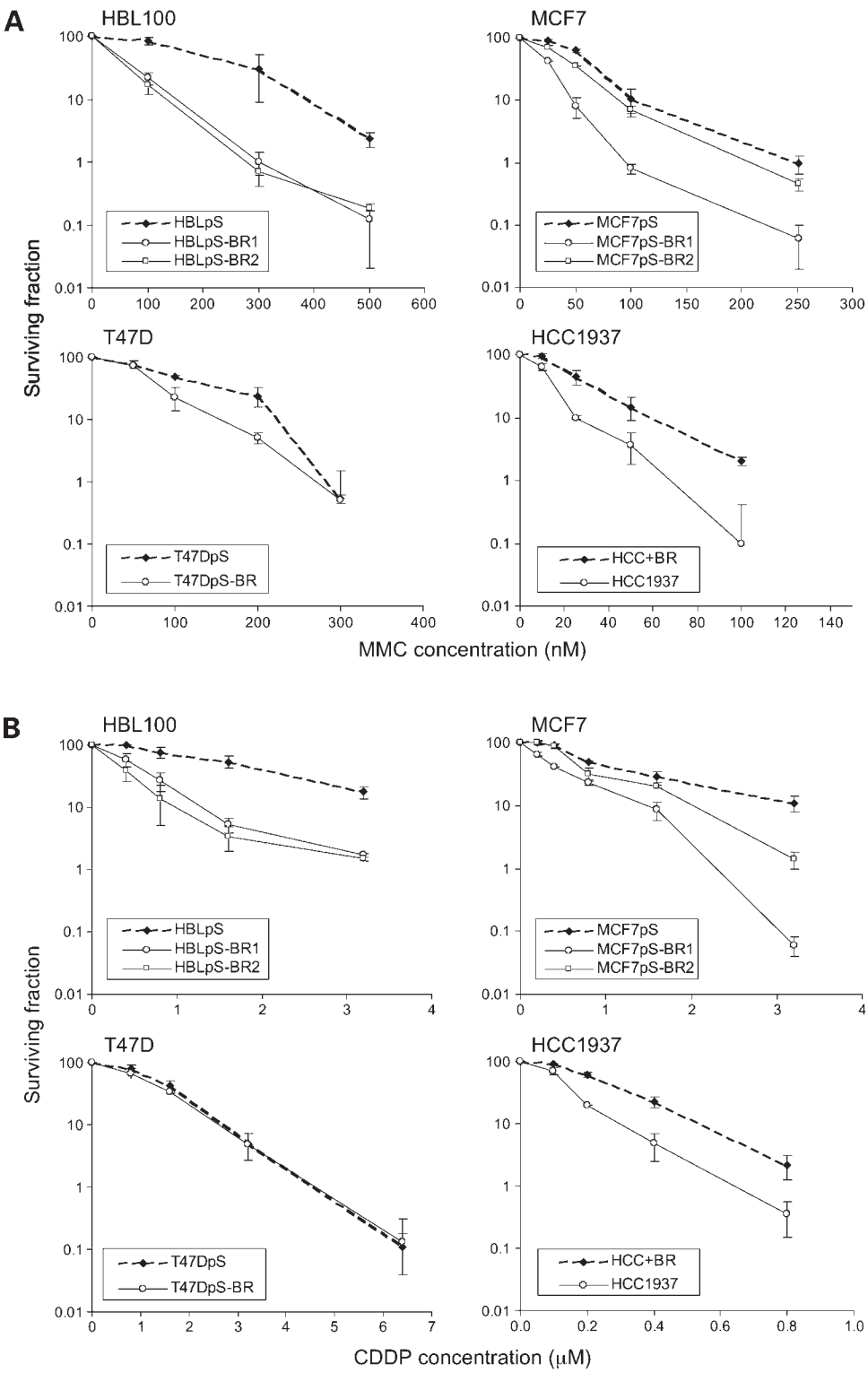

Figure 2. BRCA1 silencing sensitizes cells to ICL inducers. Clonogenic survival curves of BRCA1-proficient (--♦--, pS clones or HCC + BR) and BRCA1-deficient (–○– and –□–, pS-BR clones or HCC1937) cells. Cells were treated with increasing doses of MMC (10–500 nmol/L; *horizontal axis*; **A**) or CDDP (0.1–6.4 μmol/L; **B**) for 24 h and then allowed to grow for further 2 wk in drug-free medium. Surviving fraction (*vertical axis*) represents the mean of three independent experiments. *Bars,* SD.

Table 1. IC_{50} in BRCA1-proficent and BRCA1-deficient cells

Cell line	BRCA1*	ICLs inducers		Topoisomerase II inhibitors	
		MMC (nmol/L)	CDDP (μmol/L)	Etoposide (μmol/L)	Doxorubicin (nmol/L)
HBL100	100	238 ± 30	1.88 ± 0.06	0.91 ± 0.20	19.0 ± 5.4
HBLpS	100	240 ± 36	1.74 ± 0.33	1.20 ± 0.11	18.05 ± 4.3
HBLpS-BR1	18	84 ± 6†	0.32 ± 0.08†	0.80 ± 0.10	19.94 ± 6.2
HBLpS-BR2	16	76 ± 5†	0.44 ± 0.02†	1.10 ± 0.06	17.03 ± 7.1
MCF7	100	63 ± 7	0.99 ± 0.06	0.99 ± 0.19	22.6 ± 8,0
MCF7pS	100	69 ± 10	0.98 ± 0.04	1.18 ± 0.30	21.98 ± 5.2
MCF7pS-BR1	26	21 ± 1†	0.34 ± 0.04†	1.56 ± 0.07	10.82 ± 1.4‡
MCF7pS-BR2	53	40 ± 4	0.68 ± 0.08	1.47 ± 0.09	16.86 ± 3.4
T47D	100	96 ± 13	1.45 ± 0.25	0.15 ± 0.02	10.70 ± 2.6
T47DpS	100	100 ± 3	1.40 ± 0.31	0.16 ± 0.03	8.93 ± 2.1
T47DpS-BR	52	70 ± 10‡	1.10 ± 0.30	0.24 ± 0.04	13.26 ± 3.7
HCC1937	Null	24 ± 5	0.13 ± 0.01	0.86 ± 0.13	19.55 ± 1.5
HCC+BR	Ectopic	40 ± 3†	0.26 ± 0.01†	0.73 ± 0.12	24.73 ± 1.5

NOTE: HBLpS, MCF7pS, and T47DpS were derived from the parental cell line after transfection with scrambled pSUPER vector.
*Residual BRCA1 expression, expressed as a percentage of the value of the corresponding parental cell line.
†$P < 0.01$.
‡$P < 0.05$.

Intriguingly, after recovery, TEM was significantly higher in BRCA1-deficient cells compared with proficient ones. This observation suggests that, in the absence of BRCA1, a larger number of breaks are left unrepaired. Thus, although BRCA1 loss does not alter the ability of the cell to unhook DNA, it seems to affect the capacity to further process the damage. This conclusion was supported by the observation that after MMC challenge, different from BRCA1-proficient cells, BRCA1-deficient cells failed to efficiently produce RAD51 foci, which are required for double-strand break repair by homologous recombination (Fig. 4B). Accordingly, whereas in BRCA1-proficient cells the number of nuclei with more than five H2AX phosphorylated foci (γH2AX, a measure of the extent of double-strand breaks) raised during the treatment with MMC (0 hour) and rapidly dropped to zero during the repair phase in drug-free medium (48 hours), BRCA1-silenced cells still retained a significant fraction of γH2AX-positive nuclei at the same time point (Fig. 4C).

Role of BRCA1 in Drug-Induced Apoptosis and Senescence

Induction of apoptotic death is commonly considered the principal acute response following DNA damage. However, clinical response is indeed the result of a plethora of events, and in this context, the induction of premature senescence seems to play a major role (22, 23). To dissect the role of BRCA1 in these specific cell outcomes, apoptosis and premature senescence were comparatively evaluated in the two cell models that better responded to ICL inducers: HCC1937 and HBL100.

The increased sensitivity to CDDP and MMC showed by BRCA1-defective cells failed to correlate with increased apoptotic rate, as determined by caspase-3/7 activity, apoptotic body counting, and poly(ADP-ribose) polymerase cleavage (Fig. 5A; Supplementary Figs. S2 and S3).[2] In fact, loss of BRCA1 expression failed to result in a significant enhancement of drug-induced apoptosis in both HBL100 and HCC1937. Thus, apoptosis seems to play a minor role in BRCA1-mediated response to ICL inducers.

Intriguingly, a significant inverse correlation between BRCA1 expression and induction of premature senescence was observed. In fact, treatment with MMC or CDDP resulted in a statistically significant increase in the number of elements showing hallmarks of senescence (enlarged cytoplasm, polynucleation, senescence-associated β-galactosidase positivity, and negativity for BrdUrd incorporation) in BRCA1-defective cells compared with control cells. In contrast, no differential senescent response was observed after etoposide treatment, for which BRCA1-deficient and BRCA1-proficient cells showed comparable sensitivity (Fig. 5B; Supplementary Fig. S4A and B).[2] The phenomenon was more evident in the clones showing a higher degree of silencing, such as HBL100pS-BR1, HBL100pS-BR2, MCF7pS-BR1, and HCC1937, whereas it was barely detectable in MCF7pS-BR2 (data not shown) and T47DpS-BR clones, which exhibited only partial BRCA1 reduction after silencing (Fig. 5B). An increased propensity toward senescence was observed even under equitoxic concentrations of drugs, especially in HBL100 cells (data not shown).

Accordingly to cytologic data, BRCA1-defective cells showed also a more pronounced induction of the cyclin-dependent kinase inhibitor p21 (CDKN1A) after challenging with MMC, supporting a cell cycle arrest (Fig. 5C).

Finally, whereas karyotypic analyses indicated that the number of chromosomes per nucleus in DNA damage–recovered cells was still roughly the number of chromosomes displayed by the untreated counterpart (data not shown), cytofluorimetric analyses indicated that, after MMC challenge, BRCA1-silenced HBL100 cells tend to give rise to elements with a DNA content greater than 4N (Fig. 6A–C) that fail to incorporate BrdUrd (Fig. 6D). These results support the notion that after DNA damage BRCA1-deficient

cells tend to give rise to multinucleated elements, rather than hyperdiploid nuclei, which is also a hallmark of senescence.

Overall, our results indicate that the differential response to ICL inducers displayed by BRCA1-defective cells correlates with an increased propensity to premature senescence. Moreover, because this phenomenon was observed both in p53 wild-type (MCF7) and in p53-defective (HCC1937 and HBL100) cells, p53 seems to play

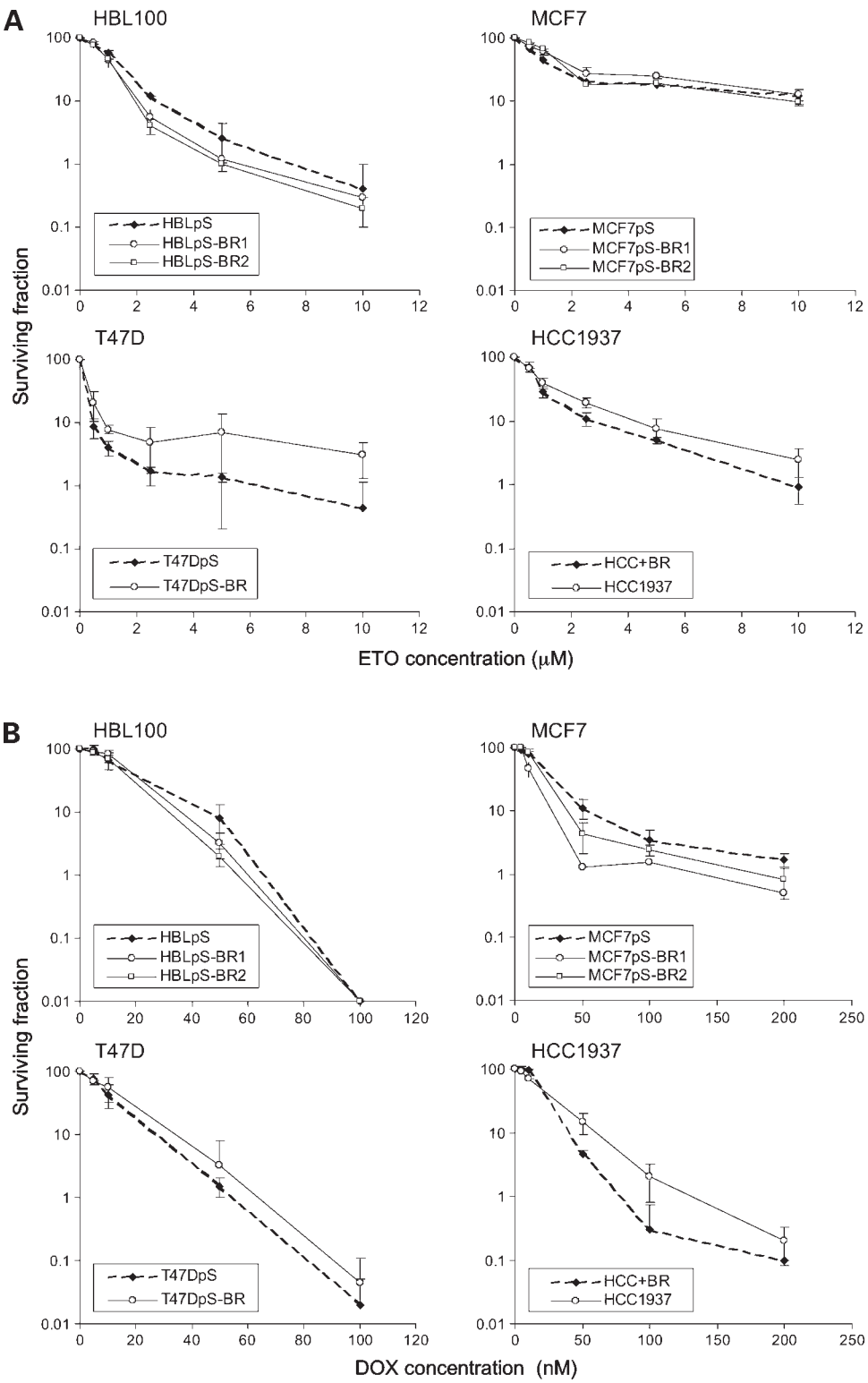

Figure 3. BRCA1 deficiency has a minor role in cell response to topoisomerase II inhibitors. Clonogenic survival curves of BRCA1-proficient (--♦--, pS clones or HCC+BR) and BRCA1-deficient (–○– and –□–, pS-BR clones or HCC1937) cells. Cells were treated with increasing doses of etoposide (*ETO*; 0.5–10 μmol/L; *horizontal axis*; **A**) or doxorubicin (*DOX*; 5–200 nmol/L; **B**) for 24 h and then allowed to grow for further 2 wk in drug-free medium. Surviving fraction represents the mean of three independent experiments. *Bars,* SD.

a minor role in premature senescence associated to BRCA1 loss.

Discussion

Tumors developed in BRCA1 mutation carriers show distinctive cytologic and molecular profiles compared with the sporadic tumor counterparts (1, 24). Nevertheless, at the moment, tailored treatments for this group of patients have only been partially investigated (12, 13). The rarity of human BRCA1-mutated cancer cell lines has further limited the exploitation of such approaches.

In the current study, we used the RNA interference technology to generate several isogenic BRCA1-silenced/nonsilenced breast cancer cell lines to assess whether a biological rational exists to implement therapeutic protocols specific for BRCA1 cancer patients. Our cell models were then challenged with several chemotherapeutics commonly used in breast cancer treatment.

We found no association between BRCA1 down-regulation and sensitivity to the topoisomerase II inhibitors etoposide and doxorubicin. Although differential response was observed in a few clones, this was not correlated to BRCA1 expression levels. Contradictory results have been published on the role of BRCA1 in modulating the response to these compounds, both *in vitro* and in clinical trials (16–18, 25–27). Other genetic variables, different from BRCA1, may account for these conflicting results. For instance, p53 mutations and topoisomerase IIα amplification have been reported to influence the response to doxorubicin of breast cancer patients (28, 29).

In contrast to topoisomerase II inhibitors, BRCA1 loss was significantly associated with increased sensitivity to ICL inducers such as MMC and CDDP, which correlated with an impaired ICL repair. The response was strictly dependent on the degree of silencing because the hypersensitive phenotype was apparent only in the cell clones that showed dramatic reduction in BRCA1 levels but was hardly appreciable in the "heterozygous-like" clones (~50% reduction). The only exception was the clone T47DpS-BR, which showed a significant hypersensitivity to MMC but not to CDDP. Several studies have either claimed or dismissed the existence of a "BRCA1 heterozygous" cell phenotype. In fact, contradictory results have been achieved about the response to DNA-damaging agents by dermal fibroblasts and lymphocytes derived from BRCA1 mutation carriers, which prevent a definitive assessment on whether the expression of only one allele affects cell behavior (30, 31). Moreover, two *in vivo* studies ruled out an increased toxicity for BRCA1 mutation carriers following either chemotherapy or radiotherapy (32, 33). Thus, whether a cellular "BRCA1 heterozygous phenotype" actually exists and whether it is recapitulated by the T47DpS-BR clone selectively under MMC challenge (but not under CDDP challenge or by the MCF7pS-BR2 clone under any stress condition) remains an open question.

The hypersensitivity to ICL inducers observed in our cell models is consistent to what previously reported for the HCC1937 cell line (in which this phenotype was reversed by ectopic restoration of BRCA1 expression) and is in line with the observation that BRCA1 defects represent favorable prognostic factors for ovarian cancer patients treated with platinum compounds (34–36).

Unexpectedly, we found that the augmented sensitivity of BRCA1-depleted cells to ICL inducers was not associated with an increased propensity to apoptosis.

Apoptosis is conventionally considered the major cell outcome after DNA damage. However, as observed in carcinomas,

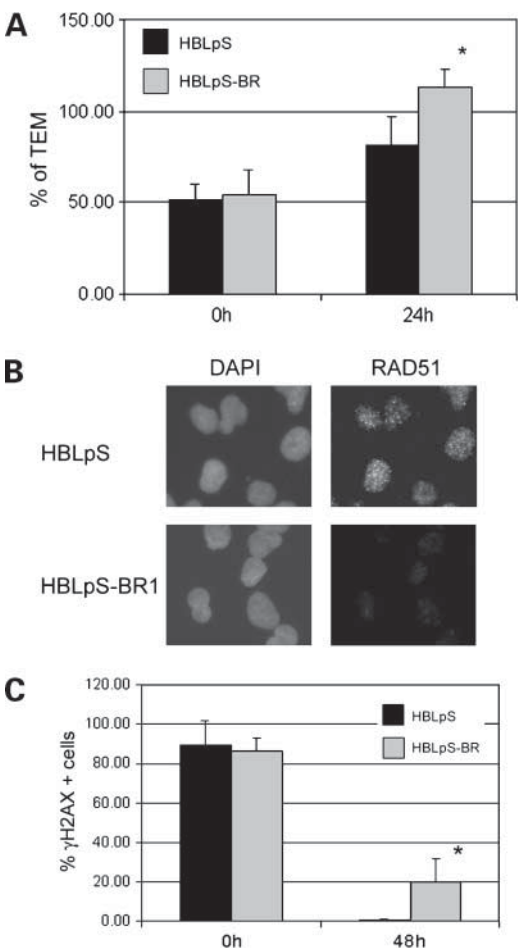

Figure 4. Hypersensitivity to ICL inducer displayed by BRCA1-silenced cells correlates with impaired repair of DNA strand breaks after ICL cleavage. **A,** alkaline Comet assay in HBLpS (*dark column*) or HBLpS-BR (*clear column*) cells after MMC treatment and radiation-induced breakage. Cells were treated with MMC (5 μmol/L) for 1 h, collected at time 0 h or after 24 h of recovery in drug-free medium (repair time), and then irradiated to shear DNA. Percentage of TEM was calculated as indicated in Materials and Methods. *, $P < 0.05$. **B,** BRCA1-silenced cells fail to induce RAD51 foci after MMC challenge. Cells were treated with MMC (0.5 μmol/L) for 24 h and then fixed and immunostained with anti-RAD51 antibodies. *DAPI,* 4′,6-diamidino-2-phenylindole. **C,** permanence of double-strand breaks in BRCA1-deficient cells after MMC-induced damage. HBLpS and HBLpS-BR cell lines were treated for 24 h with MMC and then collected right after treatment (0 h) or after a recovery time (48 h) in drug-free medium. The plot reports the percentage of cells with more than five γH2AX foci. *, $P < 0.05$.

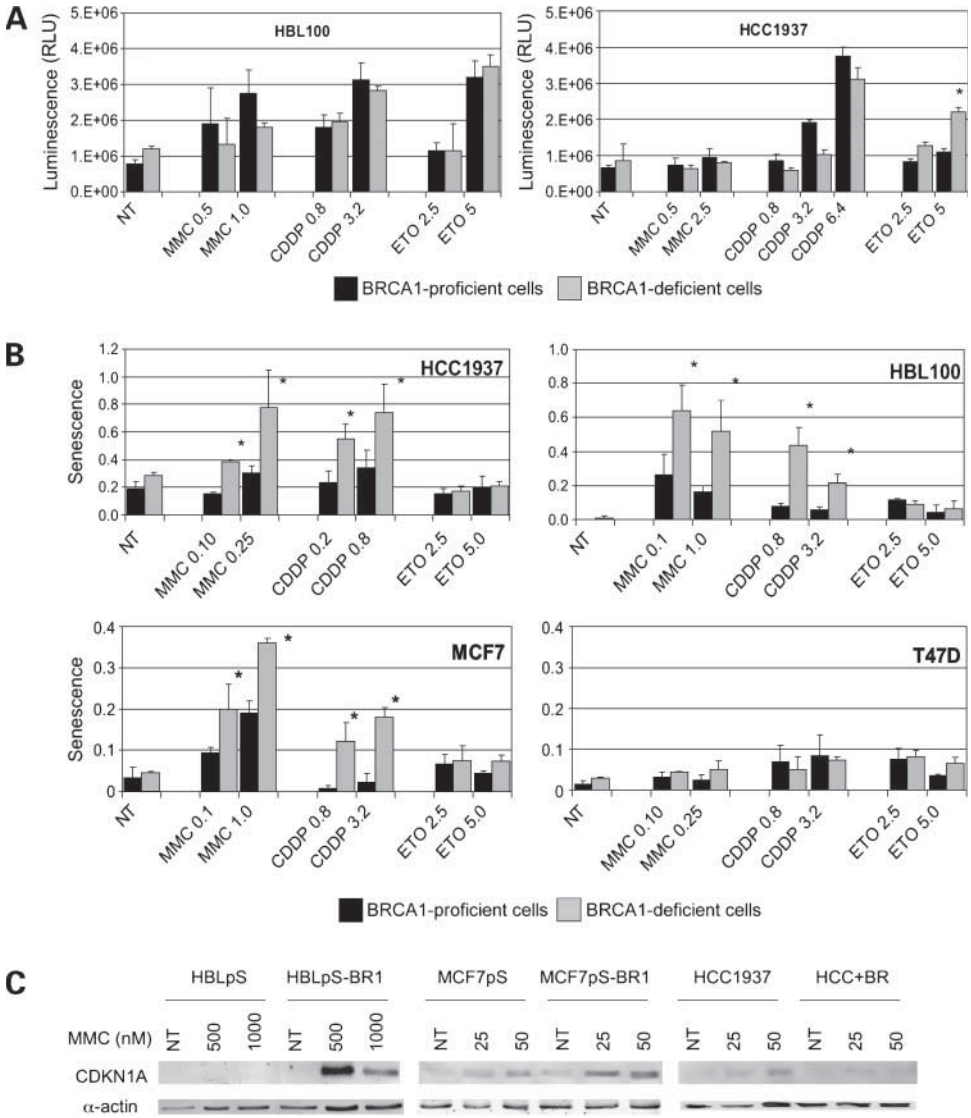

Figure 5. BRCA1 deficiency does not result in increased apoptosis but rather senescence after ICL-induced DNA damage. **A,** caspase-3/7 activity (DEVD cleavage assay) was determined by a luminescent assay and measured as relative light units (*RLU*). Scrambled vector–transfected HBLpS cells or HCC + BR (*dark column*) and silenced pS-BR clones (the mean of the two silenced clones is shown) or HCC1937 (*clear column*) were grown in duplicate on 96-well plate for 24 h and then treated with the indicated concentration of either MMC, CDDP, etoposide, or clear medium as control (*NT*) for 48 h. *, $P < 0.05$. **B,** senescent response in matched BRCA1-deficient (*light columns*) and BRCA1-proficient (*dark columns*) cells treated for 24 h in the presence of the indicated doses of MMC, CDDP, or etoposide and then left to recover for further 2 wk in drug-free medium. The fraction of senescence-associated β-galactosidase–positive cells (mean of at least three independent experiments) was calculated over the plating efficiency of untreated cells. For HBL100, the mean of the two silenced clones is shown. *Bars,* SD. *, $P < 0.05$. **C,** CDKN1A induction after MMC treatment further corroborates drug-induced growth arrest in BRCA1-silenced cells. Cells were treated for 24 h with 25 to 1,000 nmol/L of MMC, incubated in drug-free medium for 24 h, and then lysed. α-Actin was used as a loading control.

elevated doses of DNA-damaging agents tend to induce apoptosis not just as a result of DNA damage but rather as an "off-target effect" (37). Instead, an increasing body of evidence indicates that cells tend to respond to low doses of DNA-damaging agents activating a senescent pathway rather than death pathways (22, 38, 39). It has been postulated that in cells treated with cytotoxic drugs, senescence and cell death are concurrent responses characterized by different kinetics. Once the acute response (mostly death) is over, senescence distinguishes the subpopulation of growth-arrested, nonclonogenic cells from the cells that recover and proliferate normally. The overall outcome of a chemotherapeutic treatment would be therefore determined by the combination of factors responsible for acute (death) and the chronic response (senescence; ref. 22). In this regard, using a mouse lymphoma model, Lowe's group has shown that a senescence program is the major determinant in the outcome of cancer therapy *in vivo* and that this outcome is influenced by the tumor genetic background (23). Moreover, senescent cells have been actually detected in human tumors after neoadjuvant therapies (40).

On this ground, we sought to assess the senescent response in our cell models. Intriguingly, we observed that loss of BRCA1 expression significantly correlated with the induction of premature senescence after ICL-induced DNA damage. In fact, the fraction of cells arrested, polynucleated, with enlarged morphology and acidic β-galactosidase activity was significantly increased in BRCA1-deficient cells after MMC or CDDP treatment compared with BRCA1-proficient cells. Such an effect was not observed after treatment with topoisomerase II inhibitors. Thus, premature senescence seems a major response in BRCA1-defective tumor cells to ICL-induced DNA damage.

The observation that senescence is an important determinant in the response to ICL inducers in BRCA1-defective cells questions the criteria of evaluation of therapy efficacy in

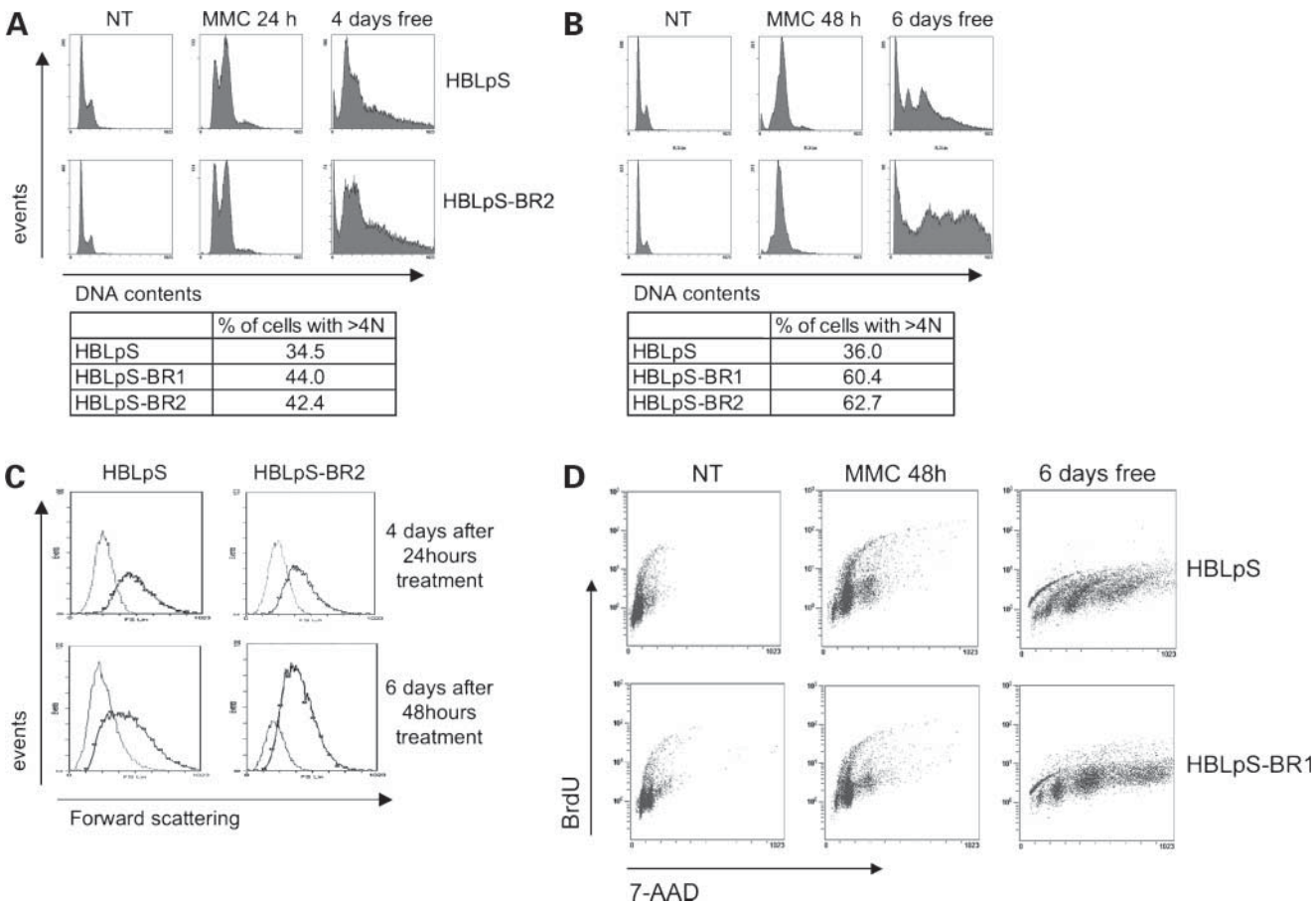

	% of cells with >4N
HBLpS	34.5
HBLpS-BR1	44.0
HBLpS-BR2	42.4

	% of cells with >4N
HBLpS	36.0
HBLpS-BR1	60.4
HBLpS-BR2	62.7

Figure 6. BRCA1 deficiency associates with accumulation of multinucleated cells after MMC treatment. **A,** cell cycle distribution analysis of propidium iodide–stained HBLpS and HBLpS-BR cells treated or not (*NT*) for 24 h with 0.5 μmol/L MMC (*MMC 24 h*) and then incubated in drug-free medium for 4 d. Table reported DNA percentage of cells with >4N DNA of one representative experiment. **B,** cell cycle distribution as in **A** of cells treated for 48 h with 0.5 μmol/L MMC (*MMC 48 h*) and then incubated in drug-free medium for 6 d. Table reported DNA percentage of cells with >4N DNA of one representative experiment. **C,** BRCA1 deficiency associates with accumulation of enlarged, hyperdiploid cells. Forward scattering of >4N DNA (*black lines*) versus <4N DNA (*gray lines*) of HBLpS and HBLpS-BR cells treated for 24 h (*top*) or 48 h (*bottom*) with 0.5 μmol/L MMC and incubated in drug-free medium for 4 and 6 d, respectively. **D,** enlarged, hyperdiploid cells are cell cycle arrested. Cells, treated as in **B**, were further incubated for 2 h with BrdUrd before analysis. DNA was labeled with 7-aminoactinomycin D (*7-AAD*) fluorescent dye.

BRCA1 mutation carriers. In fact, a senescence response, being a nonlethal strategy of "tumor cell inactivation," is more likely to result in "stable disease" rather than significant reduction of tumor burden. Thus, the Response Evaluation Criteria in Solid Tumors, conventionally used to evaluate treatment response, may not fully apply in the assessment of tumor response to CDDP/MMC-containing therapies in BRCA1 mutation carrier. In fact, these criteria are essentially based on a measure of tumor shrinkage. A reconsideration of the effectiveness of the Response Evaluation Criteria in Solid Tumors has actually started with the introduction of the so-called "molecular target therapies." In fact, targeted therapies, which act by inactivating cell signaling rather than inducing DNA damages, tend to give an acute response that hardly produces significant tumor regression, and in some instances, a senescence response has actually been reported (41). In these cases, diagnostic imaging modalities that evaluate the metabolic activity (positron emission tomography) turn out more effective (42).

Our results that BRCA1 deficiency sensitizes cells to ICL-induced senescence suggest a reconsideration of the therapeutic power of mitomycin/platinum-based treatments in BRCA1 patients and further prompt the setup of strategies for the monitoring of the senescence response *in vivo*.

Disclosure of Potential Conflicts of Interest

No potential conflicts of interest were disclosed.

Acknowledgments

We thank Dr. D.P. Harkin for the HCC1937 and HCC1937 transfected with full-length BRCA1 (HCC + BR) cell lines.

References

1. Venkitaraman AR. Cancer susceptibility and the functions of BRCA1 and BRCA2. Cell 2002;108:171–82.

2. Kim H, Chen J. New players in the BRCA1-mediated DNA damage responsive pathway. Mol Cells 2008;25:457–61.

3. Bochar DA, Wang L, Beniya H, et al. BRCA1 is associated with a human

SWI/SNF-related complex: linking chromatin remodeling to breast cancer. Cell 2000;102:257–65.

4. Silver DP, Dimitrov SD, Feunteun J, et al. Further evidence for BRCA1 communication with the inactive X chromosome. Cell 2007;128:991–1002.

5. McPherson JP, Hande MP, Poonepalli A, et al. A role for Brca1 in chromosome end maintenance. Hum Mol Genet 2006;15:831–8.

6. French JD, Dunn J, Smart CE, Manning N, Brown MA. Disruption of BRCA1 function results in telomere lengthening and increased anaphase bridge formation in immortalized cell lines. Genes Chromosomes Cancer 2006;45:277–89.

7. Aiyar S, Sun JL, Li R. BRCA1: a locus-specific "liaison" in gene expression and genetic integrity. J Cell Biochem 2005;94:1103–11.

8. Wang Y, Cortez D, Yazdi P, Neff N, Elledge SJ, Qin J. BASC, a super complex of BRCA1-associated proteins involved in the recognition and repair of aberrant DNA structures. Genes Dev 2000;14:927–39.

9. Yoshida K, Miki Y. Role of BRCA1 and BRCA2 as regulators of DNA repair, transcription, and cell cycle in response to DNA damage. Cancer Sci 2004;95:866–71.

10. Foray N, Marot D, Gabriel A, et al. A subset of ATM- and ATR-dependent phosphorylation events requires the BRCA1 protein. EMBO J 2003; 22:2860–71.

11. Yan Y, Black CP, Cao PT, et al. γ-Irradiation-induced DNA damage checkpoint activation involves feedback regulation between extracellular signal-regulated kinase 1/2 and BRCA1. Cancer Res 2008;68:5113–21.

12. Farmer H, McCabe N, Lord CJ, et al. Targeting the DNA repair defect in BRCA mutant cells as a therapeutic strategy. Nature 2005;434:917–21.

13. Lord CJ, Ashworth A. Targeted therapy for cancer using PARP inhibitors. Curr Opin Pharmacol 2008;8:363–9.

14. Sgagias MK, Wagner KU, Hamik B, et al. Brca1-deficient murine mammary epithelial cells have increased sensitivity to CDDP and MMS. Cell Cycle 2004;3:1451–6.

15. Quinn JE, Kennedy RD, Mullan PB, et al. BRCA1 functions as a differential modulator of chemotherapy-induced apoptosis. Cancer Res 2003; 63:6221–8.

16. Tassone P, Tagliaferri P, Perricelli A, et al. BRCA1 expression modulates chemosensitivity of BRCA1-defective HCC1937 human breast cancer cells. Br J Cancer 2003;88:1285–91.

17. Fedier A, Steiner RA, Schwarz VA, Lenherr L, Haller U, Fink D. The effect of loss of Brca1 on the sensitivity to anticancer agents in p53-deficient cells. Int J Oncol 2003;22:1169–73.

18. Treszezamsky AD, Kachnic LA, Feng Z, Zhang J, Tokadjian C, Powell SN. BRCA1- and BRCA2-deficient cells are sensitive to etoposide-induced DNA double-strand breaks via topoisomerase II. Cancer Res 2007;67: 7078–81.

19. Moynahan ME, Cui TY, Jasin M. Homology-directed DNA repair, mitomycin-c resistance, and chromosome stability is restored with correction of a Brca1 mutation. Cancer Res 2001;61:4842–50.

20. Hartley JM, Spanswick VJ, Gander M. Measurement of DNA cross-linking in patients on ifosfamide therapy using the single cell gel electrophoresis (comet) assay. Clin Cancer Res 1999;5:507–12.

21. Dronkert MLG, Kanaar R. Repair of DNA interstrand cross-links. Mutat Res 2001;486:217–47.

22. Chang BD, Broude EV, Dokmanovic M, et al. A senescence-like phenotype distinguishes tumor cells that undergo terminal proliferation arrest after exposure to anticancer agents. Cancer Res 1999;59:3761–7.

23. Schmitt CA, Fridman JS, Yang M, et al. A senescence program controlled by p53 and p16INK4a contributes to the outcome of cancer therapy. Cell 2002;109:335–46.

24. Foulkes WD, Stefansson IM, Chappuis PO, et al. Germline BRCA1 mutations and a basal epithelial phenotype in breast cancer. J Natl Cancer Inst 2003;95:1482–5.

25. Egawa C, Motomura K, Miyoshi Y, et al. Increased expression of BRCA1 mRNA predicts favorable response to anthracycline-containing chemotherapy in breast cancers. Breast Cancer Res Treat 2003;78:45–50.

26. Chappuis PO, Goffin J, Wong N, et al. A significant response to neoadjuvant chemotherapy in BRCA1/2 related breast cancer. J Med Genet 2002;39:608–10.

27. Goffin JR, Chappius PO, Bégin LR, et al. Impact of germline BRCA1 mutations and overexpression of p53 on prognosis and response to treatment following breast carcinoma: 10-year follow up data. Cancer 2003; 97:527–36.

28. Järvinen TA, Tanner M, Rantanen V, et al. Amplification and deletion of topoisomerase IIα associate with ErbB-2 amplification and affect sensitivity to topoisomerase II inhibitor doxorubicin in breast cancer. Am J Pathol 2000;156:839–47.

29. Geisler S, Lønning PE, Aas T, et al. Influence of TP53 gene alterations and c-erbB-2 expression on the response to treatment with doxorubicin in locally advanced breast cancer. Cancer Res 2001;61:2505–12.

30. Baldeyron C, Jacquemin E, Smith J, et al. A single mutated BRCA1 allele leads to impaired fidelity of double strand break end-joining. Oncogene 2002;21:1401–10.

31. Shorrocks J, Tobi SE, Latham H, et al. Primary fibroblasts from BRCA1 heterozygotes display an abnormal G_1/S cell cycle checkpoint following UVA irradiation but show normal levels of micronuclei following oxidative stress or mitomycin C treatment. Int J Radiat Oncol Biol Phys 2004;58: 470–8.

32. Shanley S, McReynolds K, Ardern-Jones A, et al. Late toxicity is not increased in BRCA1/BRCA2 mutation carriers undergoing breast radiotherapy in the United Kingdom. Clin Cancer Res 2006;12:7025–32.

33. Shanley S, McReynolds K, Ardern-Jones A, et al. Acute chemotherapy-related toxicity is not increased in BRCA1 and BRCA2 mutation carriers treated for breast cancer in the United Kingdom. Clin Cancer Res 2006;12: 7033–8.

34. Boyd J, Sonoda Y, Federici MG, et al. Clinicopathologic features of BRCA-linked and sporadic ovarian cancer. JAMA 2006;283:2260–5.

35. Quinn JE, James CR, Stewart GE, et al. BRCA1 mRNA expression levels predict for overall survival in ovarian cancer after chemotherapy. Clin Cancer Res 2007;13:7413–20.

36. Foulkes WD. BRCA1 and BRCA2: chemosensitivity, treatment outcomes and prognosis. Fam Cancer 2006;5:135–42.

37. Havelka AM, Berndtsson M, Olofsson MH, Shoshan MC, Linder S. Mechanisms of action of DNA-damaging anticancer drugs in treatment of carcinomas: is acute apoptosis an "off-target" effect? Mini Rev Med Chem 2007;7:1035–9.

38. Brown JM, Attardi LD. The role of apoptosis in cancer development and treatment response. Nat Rev Cancer 2005;5:231–7.

39. Berndtsson M, Hägg M, Panaretakis T, Havelka AM, Shoshan MC, Linder S. Acute apoptosis by cisplatin requires induction of reactive oxygen species but is not associated with damage to nuclear DNA. Int J Cancer 2007;120:175–80.

40. te Poele RH, Okorokov AL, Jardine L, Cummings J, Joel SP. DNA damage is able to induce senescence in tumor cells *in vitro* and *in vivo*. Cancer Res 2002;62:1876–83.

41. Hotta K, Tabata M, Kiura K, et al. Gefitinib induces premature senescence in non-small cell lung cancer cells with or without EGFR gene mutation. Oncol Rep 2007;17:313–7.

42. Benjamin RS, Choi H, Macapinlac HA, et al. We should desist using RECIST, at least in GIST. J Clin Oncol 2007;25:1760–4.